

Mitigation of Pressure Oscillations Induced by Supersonic Flow over Slender Cavities

R. A. Smith,* E. Gutmark,† and K. C. Schadow‡
Naval Air Warfare Center, China Lake, California 93555

Supersonic flow over a slender cavity excited high-frequency and high-g vibrational forces inside the cavity. The excitation of the whistle is caused by vortex shedding at the upstream end of the cavity and vortex interaction with the downstream end of the cavity associated with sound generation. The sound is fed back upstream and drives the vortex-shedding process. To suppress the acoustic whistle, an experimental test program was undertaken to characterize the acoustic cavity oscillations in a deep and narrow cavity, using microphones and flow visualization, and reduce the coherence of the vortices by geometric changes of the upstream end of the cavity. The changes that included multisteps and pins extending into the supersonic approach flow were selected to break up the orderly development of coherent vortices under acoustic excitation. With these passive shear-flow control devices, acoustic amplitude reductions by a maximum factor of 5 were obtained, essentially eliminating acoustic pressure oscillation in the cavity over the entire range of Mach numbers tested. In this article, the detailed geometric and flow parameter variation and its effect on the cavity pressure oscillations are described.

I. Introduction

ACOUSTIC oscillations inside cavities, induced by flow over the cavity, were studied extensively in the last two decades.¹⁻⁶ This phenomenon is important in subsonic and supersonic flight of airframes with cavities such as wheel wells and weapons bays, due to the excitation of structural vibrations. The oscillations are usually characterized by broadband and pure-tone components. The broadband components are primarily associated with shallow cavities, whereas deep cavities usually excite pure periodic oscillations similar to those excited by the edge-tone phenomenon. Earlier investigations¹ were aimed to quantify the sound emissions caused by cavity resonance. Later investigations attempted to develop analytical predictions for the phenomenon.^{2,3} Plumbee et al.² developed a mathematical model that was able to predict the resonant modes by relating the cavity oscillation to resonance induced by turbulent noise from the shear-layer flowing over the open end. This model was particularly successful in predicting the noise produced by deep cavities. East³ showed that some of the acoustic modes can be excited even at low subsonic Mach numbers. Over the years, different investigations proposed various theories for the excitation of the cavity pressure oscillations. Basically, most works relate these oscillations to interaction between the separated shear layer that spans across the open end of the cavities and the acoustic response of the cavity. Rossiter⁵ studied the problem experimentally in the Mach number range of 0.4–1.2 and cavity length to depth (L/D) ratios of 1–10 and concluded that an acoustic feedback is driving the oscillations. Rossiter proposed that the vortices in the shear layer that is separated from the upstream lip of the cavity, interact with the downstream lip generating acoustic pulses. These pulses propagate upstream, inside the cavity, exciting the shear layer at the upstream lip and thus enhancing the shedding of new vortices in the shear-layer. Using these arguments he devised an em-

pirical equation for the tone frequencies f

$$f = \frac{U_\infty}{L} \frac{m - \gamma}{M + (1/K)}$$

where U_∞ is the freestream velocity, L is the cavity length, m is an integer representing different modes, M is the Mach number, and K the ratio between the convection speed of the vortices and U_∞ . γ is an empirical factor related to the time lag between vortex passage and the acoustic emission. This equation was in good agreement with Rossiter's data but failed to predict results from other experiments and Mach numbers outside his range. Improved feedback models^{6,7} added the shear-layer instability and were tested for low subsonic flows over a cavity.

Block⁴ and Tam and Block⁸ questioned several points regarding these models. They claimed the mechanism of interaction between the flow instabilities and the acoustic disturbances is not treated, and there is no experimental evidence for the existence of coherent vortices in the shear layer, particularly at higher velocities. Also, the shear layer becomes stable at high Mach number, but still generates acoustic oscillations in the cavity. They proposed a different model that was related to the shear-layer oscillations at the trailing edge. During the upward motion, the flow does not interact with the cavity. However, during the downward motion, a transient high-pressure region is formed generating a compression wave, that propagates inside the cavity. Their model yielded good agreement with their data, as well as with other investigators' data in a wide range of Mach numbers. They pointed out the importance of the following parameters: the L/D ratio and the shear-layer thickness, Θ/L ratio.

Stallings and Wilcox⁹ defined a critical L/D of 10–13 that separates open-type cavities where the shear layer impinges on the trailing edge of the cavity, and a closed-type cavity, which impinges on the cavity floor; this article deals only with the first type.

Heller and Bliss¹⁰ experimentally and analytically studied the mechanism controlling pressure oscillations in shallow rectangular cavities. They related the oscillations to the unsteady motion of the shear layer that is formed over the cavity. The shear-layer interacts with the waves in the cavity to produce strong oscillations within the cavity. They showed that a slanted trailing edge and introduction of vorticity into the shear layer can suppress the oscillations.

The practical aspects of the phenomenon in airplanes are discussed in Refs. 11–13 in a Mach number range of 0.6–1.4.

Presented as Paper 90-4019 at the AIAA 13th Aeroacoustics Conference, Tallahassee, FL, Oct. 22–24, 1990; received Feb. 20, 1991; revision received Sept. 19, 1991; accepted for publication Oct. 14, 1991. This paper is declared a work of the U.S. Government and is not subject to copyright protection in the United States.

*Engineering Technician, Research Department.

†Aerospace Engineer, Research Department. Senior Member AIAA.

‡Supervisory General Engineer, Research Department.

These works also described various approaches to suppress the oscillations by passive means. The suppression devices were designed to interfere with the acoustic feedback loop. This was achieved by leading-edge spoilers and deflectors aimed to modify the shear-layer and a trailing-edge ramp. The effectiveness of the suppression devices depends on the test configuration, and was different for various frequency components.

The present report describes the work performed on a slotted-flat plate. In the first part, the parametric study of the acoustic oscillation in the flat-plate cavity is described. The following section describes the mitigation methods studied and their effect on the flat-plate resonance.

II. Experimental Arrangement

A. Freestream Producing Nozzles

Two supersonic rectangular nozzles were used for this study with Mach numbers of $M = 1.8$ and 2.6 . Most of the tests were performed at $M = 1.8$ except those discussed in relation to Fig. 15. Some of the tests were performed at off-design conditions with pressure ratios of 4.4 and 7.3. The nozzles were designed using the method of characteristics. The $M = 1.8$ rectangular nozzle had an exit dimension of 2.85×1.9 in. The momentum thickness (θ) of the boundary layer at the exit of the nozzle, on the side adjacent to the plate was 0.036 in. at a Mach number of 1.8. The wide side of the nozzle was parallel to the plane of the upper opening of the cavity. The $M = 2.6$ nozzle had an exit dimension of 3.85×2.85 in.

B. Slotted Flat-Plate

The flat plate had overall dimensions of 9.3×6 in. It was mounted parallel to the 2.85-in. side of the rectangular nozzles, flat with the nozzle's lower side. The free jet, issued from the nozzle, flows over the plate, and it is otherwise unrestricted in the other three sides.

The plate had a 8.3-in.-long and 1.4-in.-wide slot, with modular units that can be used to change the length from 1 to 8.3 in. in steps of 1 in. and the width from 0.5 to 1 in. and 1.4 in. (the slot terminates with a solid wall). The slot depth can be varied from 1 to 5 in. (Fig. 1). The upstream edge of the slot can be located at different distances from the nozzle exit. The modular units at the leading and trailing edges of the slot were used to install various suppression configurations. The relative angle between the plate and the flow was varied between 0 and 5 deg.

C. Suppression Configuration

The most effective and extensively studied configuration was the multiple pins arrangement. Most tests were performed with 0.062-in.-diam pins, with varying length between 0.2–

0.7 in. One test was done with 0.196-in.-diam pins. The number of pins, the geometric pattern, and their spacing were varied. The two most effective configurations with the minimal number of pins are shown in Fig. 1. Other suppression methods that did not yield sufficient suppression were: three steps at the upstream edge, each 0.1-in. high and 0.5-in. long, a downward 17-deg ramp, V grooves perpendicular to the stream, and streamwise grooves. Pins were also tested in the trailing-edge of the slot and a 45-deg ramp (trailing-edge corner was cut at 45 deg to the flow). With the exception of the last one, all other methods were not successful and therefore, are not described here in detail. The trailing-edge ramp was tested in combination with the pins and yielded marginal improvement.

D. Microphone Measurements

The pressure fluctuations were measured by $\frac{1}{8}$ - and $\frac{1}{4}$ -in. condenser microphones with a frequency range up to 140 kHz. The data acquisition, reduction, and spectral analysis were done using a lab computer. The microphone was located at various depths (y) and axial distances (x) along the cavity to map the amplitude and frequencies of oscillations in the entire cavity.

III. Results and Discussion

A. Flat-Plate Tests

The flat-plate tests were done to study the effect of different parameters in an idealized slot geometry. The parameters studied included 1) slot geometry; length, width, and depth; 2) microphone location; axial and lateral; 3) operational conditions of the nozzle (fully expanded and off-design); and 4) Mach number.

The first part of the tests, described in this section, were devoted to measuring the acoustic resonance frequencies and amplitudes at these different conditions. In the second part, various methods were tested to mitigate the acoustic resonance, as described in Sec. III.B.

The slot acoustics were measured at two freestream Mach numbers, 1.8 and 2.6. Most tests were performed at $M = 1.8$. An example of the acoustic pressure fluctuations spectrum in the slot, for resonance conditions, is shown in Fig. 2 for $M = 1.8$. Two resonating frequencies can be distinguished. The primary peak at 2100 Hz with an amplitude of 2.25 V and a secondary peak at $f = 1300$ Hz with an amplitude of 1.55 V. The spectrum of the pressure fluctuations inside the slot was also measured for $M = 2.6$ (not shown here). The frequency peak at $f = 1200$ Hz increased from 1.5 V for $M = 1.8$ to 3.5 V at $M = 2.6$ (not shown here). The peak at the frequency of 2100 Hz remained unchanged. The frequency and amplitude of the resonance modes are dependent on the various parameters as discussed in the following sections.

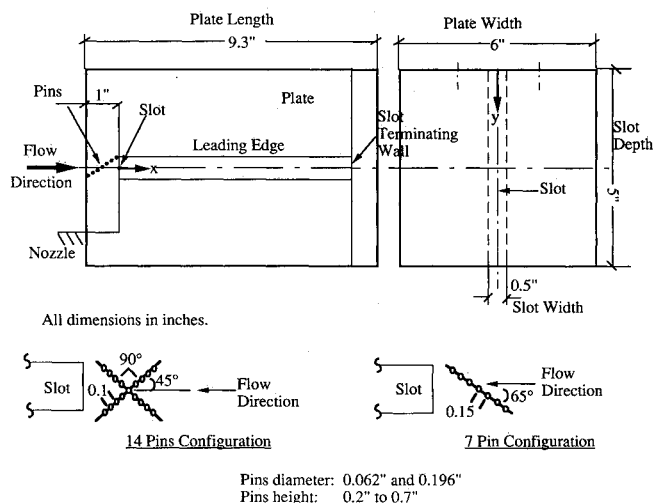


Fig. 1 Experimental setup.

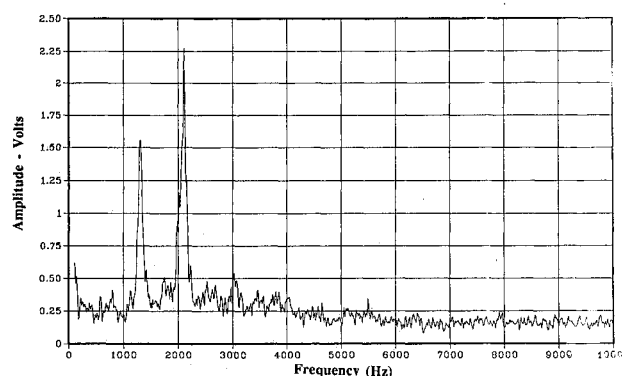


Fig. 2 Spectrum of pressure oscillations in a slender cavity of $L/D = 1.465$, $D = 5$ in., $W = 0.5$ in. High peaks correspond to 1st and 2nd modes. Microphone at $X/L = 0.09$ and $Y/D = 0.6$ Freestream Mach $M = 1.8$.

1. Effect of Slot Length (L)

Figure 3 shows the variation of frequency and amplitude with the slot length, for a slot width of $W = 0.5$ in. and depth of $D = 2$ in. The figure shows both primary (or major) and secondary (minor) peaks. The resonance frequency drops monotonically with increasing L (except between $L = 5$ and 7.3 in.). A maximal amplitude is detected for $L = 3$ in. There are two dominant resonating modes and their relative amplitudes change for different slot lengths.

Similar behavior of the frequency was measured for a different slot geometry with 0.5 in. width and 5 in. depth (Fig. 4). The amplitude of the different modes is shown in Fig. 5. The highest level was measured for a slot length of $L = 7.3$ in. A lower local maximum was also obtained for $L = 4$ in.

2. Effects of Slot Width (W)

Three slot widths were tested: 0.5, 1, and 1.4 in. In general, there were no significant differences between them (either in

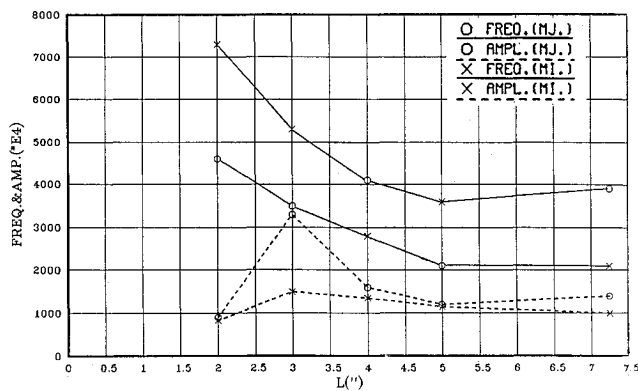


Fig. 3 Effect of slot length on amplitude and frequency: $W = 0.5$ in.; $D = 2$ in.; microphone = 0.5, 1 in.

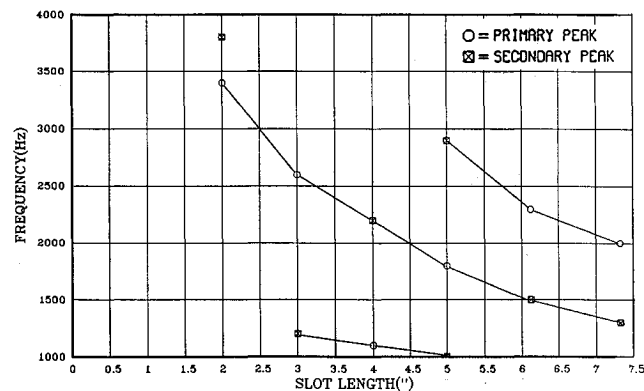


Fig. 4 Effect of slot length on frequency: microphone—0.5, 3 in.; $D = 5$ in.; $W = 0.5$ in.

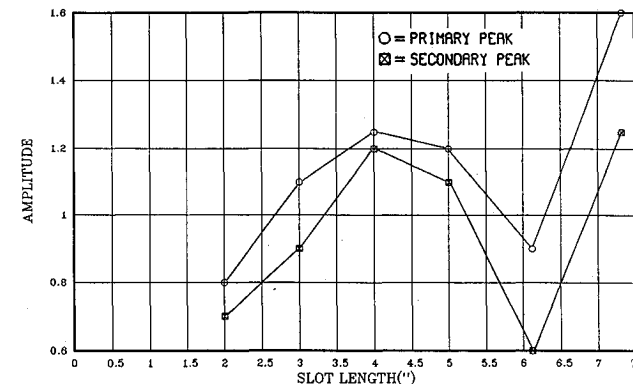


Fig. 5 Effect of slot length on amplitude: microphone = 0.5 in., 3; $D = 5$ in.; $W = 0.5$ in.

resonance frequencies or in amplitude). There were two exceptions for a slot depth of 2 in. and length of 3 in. where the narrowest slot had the highest amplitude. Similar results were measured for a slot of $L = 3$ in. and $D = 1$ in.

3. Effect of Slot Depth (D)

The variation of the resonance amplitude with the slot depth is shown in Fig. 6 for different slot lengths. The general pattern shows an increased amplitude with depth, except for the shortest slot of $L = 2$ in.

Most of the measurements in this work were done with $D = 5$ in.

4. Microphone Location

The amplitude of the pressure fluctuations distribution in the slot was mapped in the axial (x) and depth (y) directions. The mapping was done in a $L = 5$ in., $W = 0.5$ in., and $D = 5$ in. slot. The measurements could be performed only in the upstream half of the slot due to high-flow loads at the downstream section. The variation of the amplitude of three different resonance frequencies: 1000, 1800, and 3000 Hz along the slot length (x direction) is shown in Fig. 7 for three depth locations ($y = 2, 3$, and 4 in.). The depth of the measurements did not have a substantial effect in most of the conditions measured. One exception was a frequency of 3000 Hz in the slot center where the amplitude reduced drastically with increasing microphone depth (Fig. 8).

The amplitude of the 1000 Hz resonance was nearly independent of the axial location, whereas the other two showed significant variation with a minimum level at the slot quarter length for 3000 Hz, and a minimum at the center for 1800 Hz. Most measurements were performed with the microphone located at $x = 0.5$ in. and $y = 3$ in.

5. Effect of Operating Conditions

The flow over the slotted flat plate was generated by a rectangular nozzle that was designed for a fully expanded

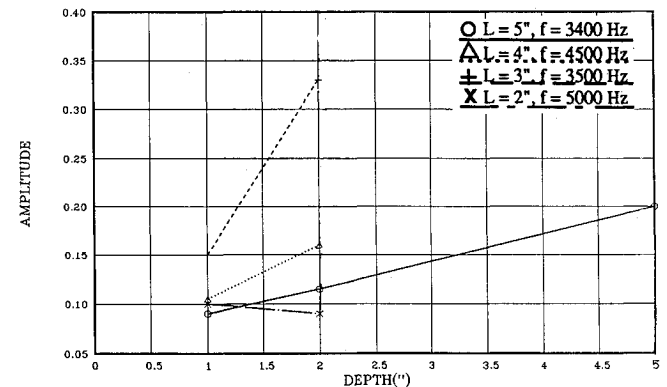


Fig. 6 Effect of slot depth on amplitude: $W = 0.5$ in.; microphone = 0.5 in., 1 in.

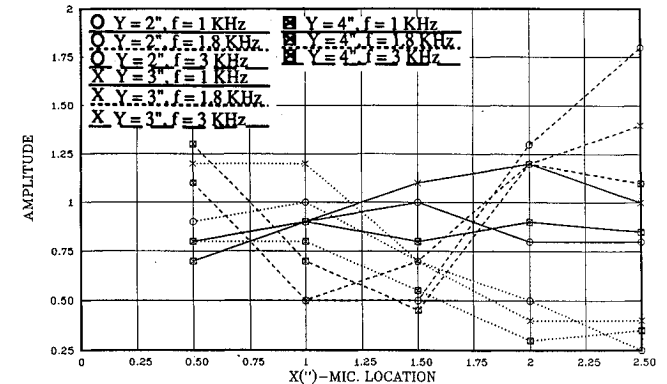


Fig. 7 Effect of axial microphone location in slot: $L = 5$ in.; $W = 0.5$ in.; $D = 5$ in.

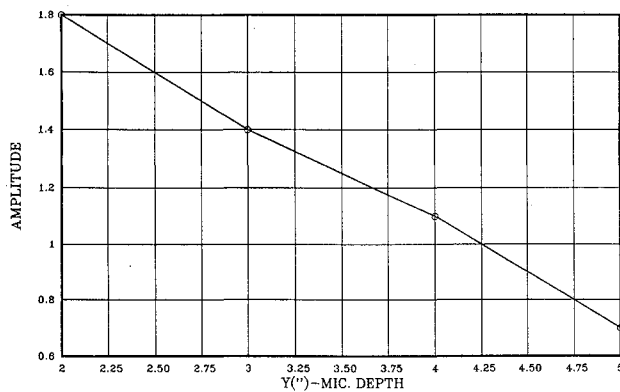


Fig. 8 Effect of microphone depth: $W = 0.5$ in.; $D = 5$ in.; X (microphone) = 2.5 in.; $f = 3$ kHz; $L = 5$ in.

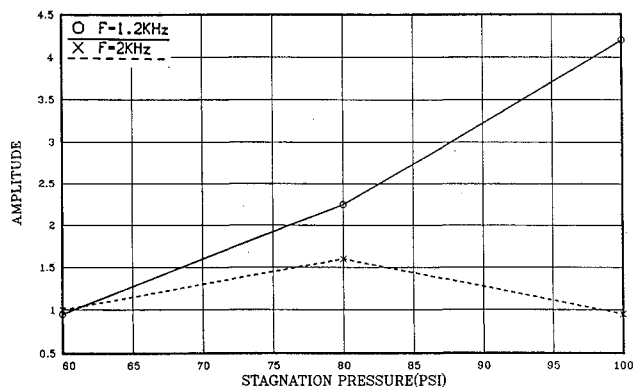


Fig. 9 Effect of nozzle operating conditions: $L = 7.3$ in.; $D = 5$ in.; $W = 0.5$ in.

operation at $M = 1.8$ (stagnation pressure = 80 psi) (or $M = 2.6$ in some tests). The effect of stagnation pressure on the slot resonance was checked for over and underexpanded conditions corresponding to pressure ratios of 4.4 and 7.3. The fully expanded Mach numbers for these conditions are 1.62 and 1.96. Figure 9 depicts the variation of the resonance amplitude with the chamber stagnation pressure. There was no significant difference between overexpanded and design conditions. However, for a resonance frequency of $f = 1200$ Hz, the underexpanded conditions yielded more than four times higher amplitude relative to the design conditions.

6. Dependence of Strouhal Number and Comparison to Previous Data

Theoretical works and previous experimental results showed that the resonance frequency in the slot can be presented as a nondimensional parameter (Strouhal number $St = f \cdot L/U$) when normalized by the slot length (L) and the free stream velocity (U). The present measurement results for the different L/D ratios, from 0.4 to 3.65, two slot depths of 2 and 5 in. and two Mach numbers 1.8 and 2.6 are presented in their nondimensional form in Fig. 10. The present data is compared with computed curves that are based on theoretical empirical models by Rossiter,⁵ Tam and Block,⁸ and Bilanin and Covert.⁷ Due to the scatter in the data, it is difficult to have a valid comparison with the various models. However, extrapolation of Tam and Block's model seems to yield the best agreement with the present data.

The scatter in the nondimensional data, could suggest that the normalizing parameters L and U are not sufficient to describe the acoustic resonance in the slot.

B. Mitigation of the Pressure Oscillations in the Flat-Plate

The separation of the shear layer at the leading edge of the cavity was determined to be a crucial point for the acoustic excitation inside the cavity.^{5,7,8} The various mitigation tech-

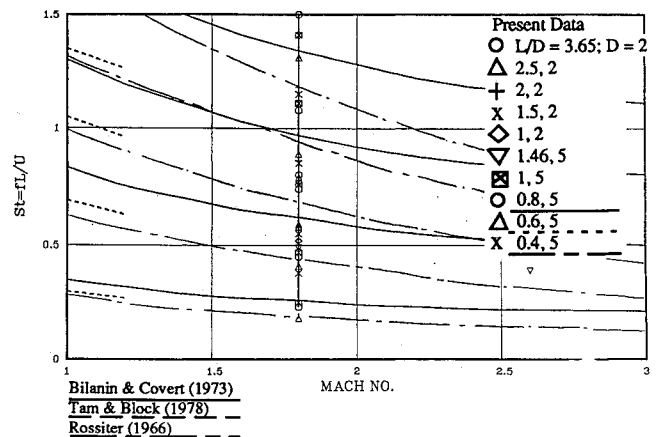


Fig. 10 Comparison of the Strouhal numbers of different instability modes in duct to theoretical predictions.^{5,7,8}

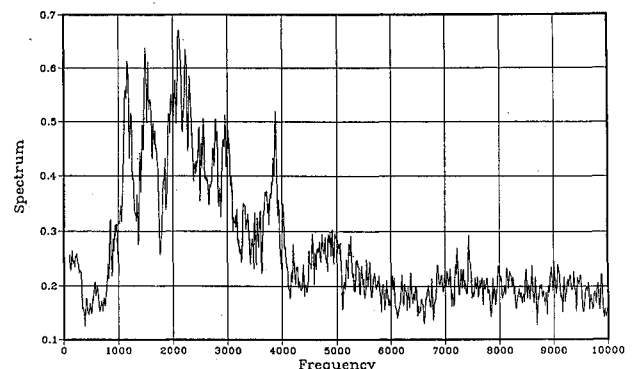


Fig. 11 Spectrum of the suppressed pressure oscillations by leading-edge pins. The cavity geometry and test conditions are identical to Fig. 2.

niques tested were aimed at modifying the boundary layer upstream of the leading edge, such that the shear-layer instability is altered. Other methods modified the trailing edge of the slot to reduce the feedback.

The various methods included small pins, steps, ramp, grooves in the leading edge, and pins and ramp at the trailing edge. The most effective and most extensively studied configuration were the pins in the leading edge. Many configurations of pins were tested and the pins' angle, diameter, height, location, and spacing were optimized. The most effective configuration with the minimal number of pins was seven, 0.062-in.-diam pins installed at an angle between 30–45 deg relative to the freestream flow, upstream of the leading edge. The spectrum measured in the slot for the same conditions as in Fig. 2, but with the seven pins is shown in Fig. 11. The peak frequency was suppressed by more than five times, to nearly the background noise level.

Schlieren spark photographs comparing the flow over the cavity without and with pins are shown in Figs. 12a and b, respectively. The photographs show that the main effect of the pins is to produce a thick turbulent boundary layer over the slot that is likely to suppress the generation of coherent vortices and reduce the flapping of the shear layer over the cavity.

1. Effect of Pin Heights (H)

Most tests were performed with 0.062-in.-diam pins. Their height was varied from 0.2 to 0.7 in. (Fig. 13). The effectiveness of the pins grows gradually until saturation for $H > 0.5$ in. Most of the tests were performed using this height.

A single test was performed with four thicker pins of 0.196-in. diam. The suppression level was similar to that of the standard seven pins of 0.062-in. diam.

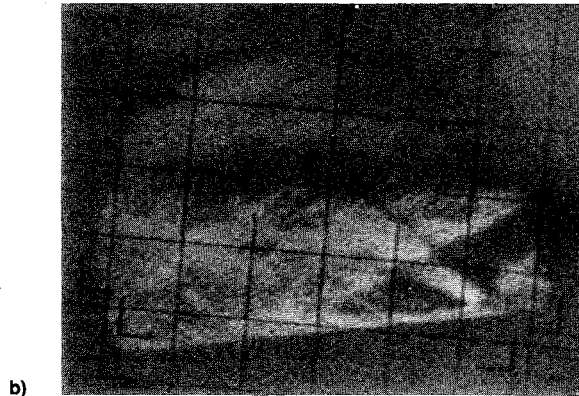
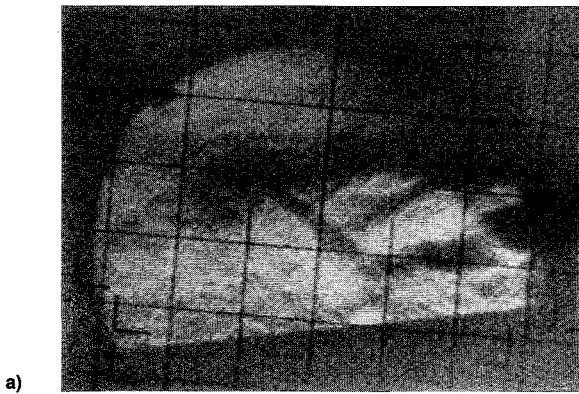


Fig. 12 Schlieren spark photograph of the flow over the cavity; a) flat plate only, and b) with 14 pins at the leading edge of the slot.

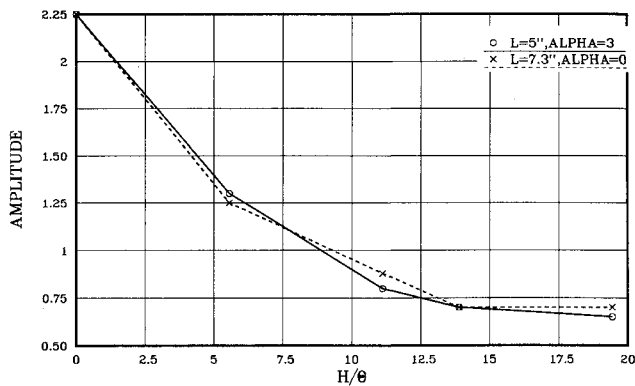


Fig. 13 Effect of pin heights: $W = 0.5$ in.; $D = 5$ in.; microphone = 0.5 in., 3 in.

2. Effect of Pin Spacings (S)

A single test was performed with every second pin removed from the seven pins configuration, yielding a more spaced four-pin row at an angle to the flow. The pins effectiveness was significantly reduced and the oscillations amplitude was almost unaffected.

3. Effect of Angle-of-Attack (α)

Most of the tests were done with a zero angle-of-attack of the plate relative to the flow. The effectiveness of the seven pins configuration was measured at 3° . Figure 14 shows that without pins, the amplitude of oscillations increased more than twice. With the pins, there was no difference between 0 – 3 -deg angle-of-attack, the suppression was equally effective.

4. Effect of Mach Number

Suppression by 14-pin configuration, arranged in an X shape, where each leg is at 45° deg to the flow, was measured for Mach numbers of 1.8 and 2.6 . The oscillations level without

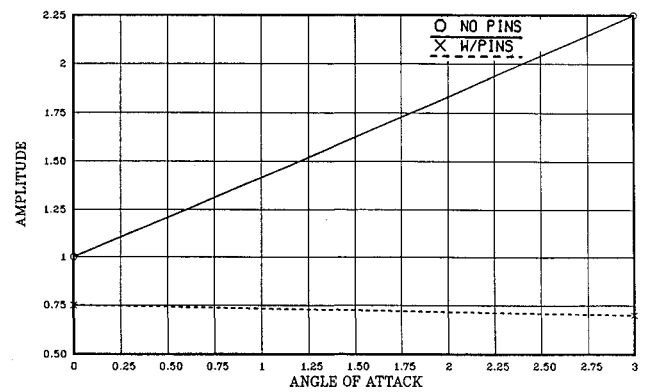


Fig. 14 Effect of angle-of-attack: $L = 5$ in.; $W = 0.5$ in.; $D = 5$ in.; microphone = 0.5 in., 3 in.

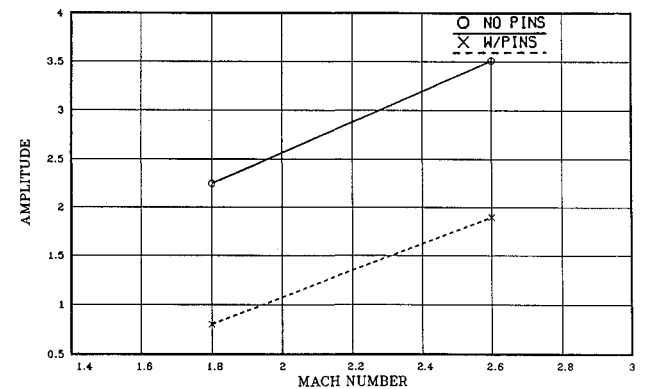


Fig. 15 Effect of Mach number: $L = 7.3$ in.; $W = 0.5$ in.; $D = 5$ in.; microphone = 0.5 in., 3 in.; 14 pins in an X configuration.

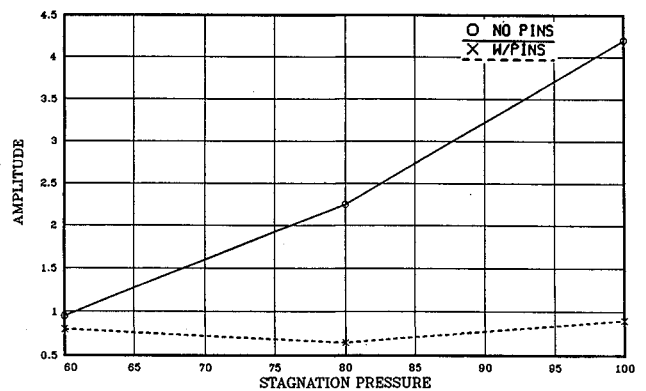


Fig. 16 Effect of pins at design and off-design conditions: $L = 7.3$ in.; $W = 0.5$ in.; $D = 5$ in.; microphone = 0.5 in., 3 in.

and with pins is depicted in Fig. 15. The suppression was equally effective for both Mach numbers studied.

5. Effect of Operating Conditions

It was shown in Fig. 9 that when the freestream nozzle is operating at underexpanded conditions, the amplitude of oscillations is increased considerably. The effectiveness of the pins suppression was checked under these conditions (Fig. 16), and yielded similar reduction of oscillations in the entire range of stagnation pressure measured.

6. Effect of Distance Between Pins and Slot

The location of the pins relative to the slot, had an effect on the suppression effectiveness, depending on the pins height. For small pins (0.3 -in.) there was a high sensitivity to the pins location: the pins were effective only when a gap of 0.5 in. separated them and the slot, for higher pins the difference was insignificant. However, when the gap between the pins

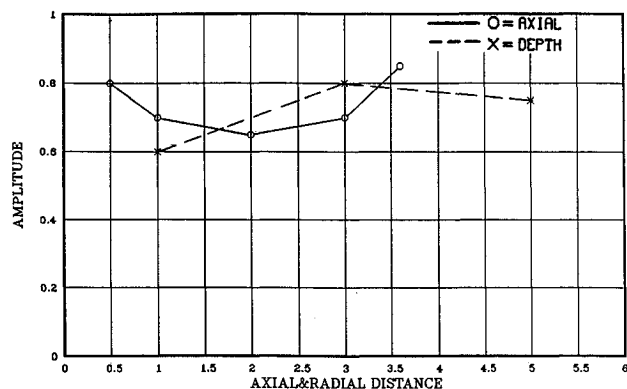


Fig. 17 Uniformity of suppression in slot: $L = 7.3$ in.; $W = 0.5$ in.; $D = 5$ in.; microphone = 0.5 in., 3 in.

and the slot was closer to 1 in., the effectiveness of the pins was reduced.

7. Uniformity of Suppression

As shown in Figs. 7 and 8, the amplitude of the pressure fluctuations in the slot varies with the location along and inside the slot. It was important to check the amplitude of the suppressed pressure fluctuations at different locations in the slot. Figure 17 shows two scans inside the slot in the axial (x) and radial (y) (depth) directions. The suppression was uniform in the entire slot area.

8. Combination of Pins and Trailing-Edge Ramp

A single test was performed with a combination of 16 pins in an X configuration and a 45-deg ramp at the trailing edge. A marginal improvement over a "pins only" configuration was measured.

IV. Summary

The source of vibrations in a narrow cavity was studied to quantify the phenomenon and to devise suppression methods. It was assumed, based on previous evidence, that the source of the vibrations is an acoustic resonance in the cavity caused by interaction between the freestream flow and the duct acoustics.

A parametric study was conducted using a slotted flat plate. The amplitude and frequency of the acoustic resonance were shown to be dependent on the slot dimensions, location in the slot, freestream Mach number, and nozzle operating conditions. Comparison with theories that predict the normalized frequency (Strouhal number) yielded only qualitative agreement.

Various techniques were tested to interfere with the excitation source of the acoustic oscillations. The most effective ones were small pins installed upstream of the slot, that cause disturbance in the boundary layer of the freestream flow just before separation at the leading edge of the slot, thus interfering with the formation of coherent structures in the separated shear layer. A configuration of seven 0.062-in.-diam pins, 0.5-in. long, almost completely suppressed the oscillations at freestream Mach numbers of $M = 1.8$ and 2.6, even for high excitation level caused by the screech when the nozzles were operated at underexpanded conditions. The suppression was uniform in the entire slot area.

References

- ¹Roshko, A., "Some Measurements of Flow in a Rectangular Cut-out," NACA TN-3488, Aug. 1955.
- ²Plumbee, H. E., Gibson, J. S., and Lassiter, L. W., "A Theoretical and Experimental Investigation of the Acoustic Response of Cavities in an Aerodynamic Flow," USAF Rept. WADD-TR-61-75, OH, March 1962.
- ³East, L. F., "Aerodynamically Induced Resonance in Rectangular Cavities," *Journal of Sound and Vibration*, Vol. 3, March 1966, pp. 277-287.
- ⁴Block, J. W., "Measurements of the Tonal Component of Cavity Noise and Comparison with Theory," NASA TP-1013, Nov. 1977.
- ⁵Rossiter, J. E., "Wind Tunnel Experiments on the Flow Over Rectangular Cavities at Subsonic and Transonic Speeds," Reports and Memoranda 3438, Aeronautical Research Council, London, Oct. 1966.
- ⁶DeMetz, F. C., and Farabee, T. M., "Laminar and Turbulent Shear Flow Induced Cavity Resonances," AIAA Paper 77-1293, Oct. 1977.
- ⁷Bilanin, A. J., and Covert, E. E., "Estimation of Possible Excitation Frequencies for Shallow Rectangular Cavities," *AIAA Journal*, Vol. 11, No. 3, 1973, pp. 347-351.
- ⁸Tam, C. K. W., and Block, P. J., "On the Tones and Pressure Oscillations Induced by Flow Over Rectangular Cavities," *Journal of Fluid Mechanics*, Vol. 89, No. 2, 1978, pp. 373-399.
- ⁹Stallings, R. L., and Wilcox, F. J., "Experimental Cavity Pressure Distributions at Supersonic Speeds," NASA TP 2683, June 1987.
- ¹⁰Heller, H. H., and Bliss, D. B., "The Physical Mechanism of Flow Induced Pressure Fluctuations in Cavities and Concepts for Their Suppression," AIAA Paper 75-491, March 1975.
- ¹¹Shaw, L. L., "Suppression of Aerodynamically Induced Cavity Pressure Oscillations," *Journal of Acoustical Society of America*, Vol. 66, No. 3, 1979, pp. 880-884.
- ¹²Shaw, L. L., Bartel, H., and McAvoy, J., "Acoustic Environment in Large Enclosures with a Small Opening Exposed to Flow," *Journal of Aircraft*, Vol. 20, No. 3, 1983, pp. 250-256.
- ¹³Shaw, L. L., Clark, R., and Talmadge, D., "F-111 Generic Weapons Bay Acoustic Environment," *Journal of Aircraft*, Vol. 25, No. 2, 1988, pp. 147-153.